

DC/DC Full-bridge Converter for Cathodic Protection Application with Phase-Shift Control Method and No Auxiliary Circuit

Shokoufeh Valadkhani

*Department of Electrical Engineering
Amirkabir University of Technology
(Tehran Polytechnic)
Tehran, Iran
sh.valadkhani@aut.ac.ir*

Mojtaba Mirsalim

*Department of Electrical Engineering
Amirkabir University of Technology
(Tehran Polytechnic)
Tehran, Iran
mirsalim@aut.ac.ir*

Amir Khorsandi

*Department of Electrical Engineering
Amirkabir University of Technology
(Tehran Polytechnic)
Tehran, Iran
a_khorsandi@aut.ac.ir*

Abstract—Cathodic protection (CP) DC/DC converters are the external power sources used in CP systems to convert fix DC voltage to variable DC output voltage and bring about variable output current as well. In low to medium output voltages, where the duty cycle is less than 30%, zero voltage switching (ZVS) is unattainable. Therefore, a switching control method which is the combination of ZVS and variable frequency pulse width modulation (VFPWM) is proposed in this paper. Using the proposed method, the DC/DC full-bridge converter can operate under a wide range of output voltage from 0 to 75V and output current from 0 to 25A with high efficiency. Simulation results demonstrate the accuracy of this method.

Index Terms—Cathodic protection, DC/DC full-bridge, Zero voltage switching, Variable frequency pulse width modulation, Variable DC output power.

I. INTRODUCTION

The principle of cathodic protection (CP) is to make the potential of the whole surface of the steel structure sufficiently negative with respect to the surrounding environment to ensure that no current flows from the metal into the medium. This can be done by forcing an electric current to flow through the electrolyte (i.e., soil or sea water) towards the surface of the metal to be protected. Cathodic protection DC/DC converters convert fixed DC voltage to variable DC output power [1], [2]. Full-bridge converters with phase-shift switching control have been widely employed in high-power applications. By using zero voltage switching (ZVS) control, transistor voltage becomes zero before the controller turns the MOSFETs on. Thus, the switching loss can be significantly reduced. However, under light-load conditions, the ZVS is not maintained due to the small current flowing in the circuit of the phase-shift converter, which is needed to discharge the parasitic capacitors. Several methods have been proposed to extend ZVS range to improve the efficiency of the phase-shift-controlled full-bridge converters [3]–[7]. All these topologies require auxiliary components to increase the converter efficiency in a wide range of load current which results in a more conduction loss, higher design cost, and more complicated circuit, which is not economical. To overcome this problem, some methods have been proposed

in the literature to extend the ZVS range without additional auxiliary components [8]–[10]. A new control method was proposed in [8], which uses a variable delay time of lagging-leg switches under light load conditions. By increasing the delay time, switching occurs at a lower drain-source voltage, and the switching losses can be reduced under light load conditions without auxiliary components and side effects on heavy load conditions. Another optimization method to improve the efficiency by tuning magnetizing and commutation inductors has also been introduced in [9].

Other studies focus on a combination of different power converter topologies and hybrid converters or LLC resonant converter to solve the problem [11]–[14]. These topologies can operate under a wide range of output voltages. However, the disadvantages of these methods include having complicated control strategy, more components, and higher cost. In all of the converters proposed in the literature, the output voltage and current is constant, but for CP in which the output voltage, current, and power should be changed by the user demand, achieving a ZVS at low-output powers is actually unattainable. Therefore, a control strategy which is the combination of two modes, the ZVS and variable frequency pulse width modulation (VFPWM), is proposed in this paper to achieve all the requirements of the user and still provide high efficiency in both light and high loads. The DC/DC full-bridge converter is designed for different outputs up to 75V and 25A. In section II, the circuit configuration of the proposed converter is explained and operational principles of ZVS and VFPWM modes are discussed. Moreover, the control strategy of the full-bridge converter is introduced and described in section II. The Simulation results are presented in section III. Finally, conclusions are drawn in Section IV.

II. PROPOSED DC/DC FULL-BRIDGE CONVERTER

In this section, a DC/DC full-bridge converter with 400V DC input and 0 to 75V DC output voltage and 0 to 25A output current is designed in particular for high efficiency at low output voltages, practically used in CP applications. Fig.

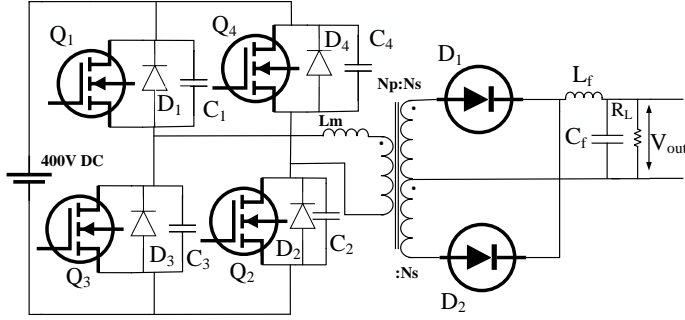


Fig. 1. DC/DC full-bridge converter.

1 illustrates the DC/DC converter composed of the primary switches $Q_1 \sim Q_4$, a high-frequency transformer with at most $21kHz$ operating frequency, output rectifier diodes, and an LC output filter. As the output power is controlled by the user, the ZVS is hard to achieve especially in low output power.

The proposed control method consists of two parts: a VFPWM in light outputs and a ZVS in high output powers to achieve a nearly flat, high efficiency in a wide operating range of output current. This high, flat efficiency versus output power curve is one of the main requirements of CP converters [2]. With this in mind, following considerations are studied to find the ideal and functional range of VFPWM and ZVS modes.

A. Principle of ZVS Mode

Fig. 2 shows the waveforms of primary-side voltage (V_{pri}), current (I_{pri}), and secondary-side voltage (V_{sec}), respectively. At time t_2 , switch Q_4 turns off and primary current charges the output capacitance of Q_4 and discharge the output capacitance of Q_2 , turning on the diode D_2 . After D_2 starts conducting, Q_2 can be turned on with almost no voltage applied across it. To achieve ZVS, the energy stored in the leakage inductance has to be larger than the energy stored in the output capacitances. The same is true for Q_4 at t_6 .

At time t_5 , switch Q_1 turns off and primary current charges the output capacitance of Q_1 and discharge the output capacitance of Q_3 , turning on the diode D_3 . After D_3 starts conducting, Q_3 can be turned on with almost no voltage applied across it. In this case, when Q_1 turns off, the primary current of the transformer is the reflected output current. The energy of the large filter inductor in the secondary is used to achieve ZVS. Therefore, the ZVS is achieved easily for switches Q_1 or Q_3 .

The mechanism by which ZVS is achieved is different for both legs of the full-bridge. For Q_2 and Q_4 , the ZVS is provided by the resonance between the leakage inductance L_{lk} and the output capacitance of the switches. Before Q_2 is turned off, (I_{pri}) is circulating through D_3 and Q_2 , and the primary voltage is clamped to zero. When Q_2 turns off, (I_{pri}) forces the diode D_4 to turn on and the energy remaining in

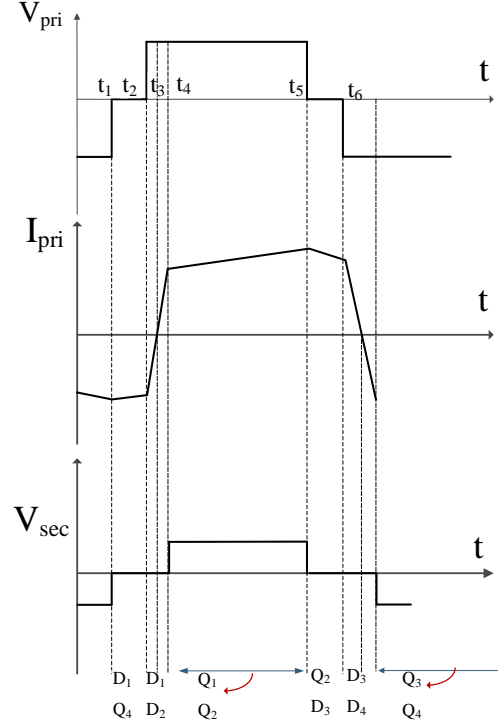


Fig. 2. Waveforms of primary-side current (I_{pri}) and voltage (V_{pri}), and secondary side voltage (V_{sec}).

the leakage inductance returns to the source. In order to turn on D_4 , the output capacitance of Q_4 has to be discharged and the output capacitance of Q_2 charged to the input voltage. The energy available for discharging the output capacitance of Q_4 and charging the output capacitance of Q_2 is the energy stored in L_{lk} after t_2 or t_6 . The required energy in the leakage inductance is [15], [16]:

$$E = \frac{1}{2}L_{lk}I_2^2 > \frac{4}{3}C_{MOS}V_{in}^2 + \frac{1}{2}C_TV_{in}^2 \quad (1)$$

where, L_{lk} is the transformer leakage inductance, C_{MOS} is the switch output capacitance, C_T is the transformer winding capacitance, I_2 is the primary current of the transformer at t_2 or t_6 , and V_{in} is the input voltage. The ZVS for Q_2 and Q_4 depends on the load of the converter. At light loads, therefore, the current through L_{lk} at t_2 or t_6 may not be sufficient to charge or discharge the output capacitances of the switches and to turn on the antiparallel diodes (D_2 and D_4).

In order to ensure that Q_4 will turn on with zero voltage, a dead time is needed between the turn-off of Q_2 and the turn-on of Q_4 to ensure that D_4 conducts prior to turn on of Q_4 . However, with a long dead time, the output capacitor of the switch will discharge and continue to resonate and then drop. The needed magnetization inductance of the transformer can

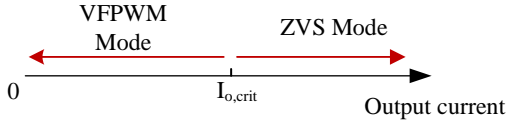


Fig. 3. Transition point of the proposed switching control method.

be calculated as: [15]

$$L_M > \frac{nDV_{in}}{4\Delta I_O f_s} \quad (2)$$

where, n is transformer turns-ratio, D is the duty cycle of switches, f_s is the switching frequency, and ΔI_O is the output current change that is considered as:

$$\Delta I_O = 0.1I_O. \quad (3)$$

here, I_O is the average output current.

B. Zero Voltage Switching Range

At light loads, the ZVS for Q_1 and Q_3 can be achieved, as D_1 and D_3 can always be turned on by the reflected current of the output filter inductance. Nonetheless, ZVS conditions for Q_2 and Q_4 are only achieved for load currents above the critical value. The required critical current in the primary side to attain ZVS is: [15], [16]

$$I_{crit} = \sqrt{\frac{2}{L_{lk}} \left(\frac{4}{3} C_{MOS} V_{in}^2 + \frac{1}{2} C_T V_{in}^2 \right)}. \quad (4)$$

The current through L_{lk} at t_2 is:

$$I_2 = \frac{N_P}{N_S} I_o + \frac{\Delta I_o}{2} - \frac{V_{out}}{L_f} (1 - D) \frac{T}{2} \quad (5)$$

where, L_f is the filter inductance, V_{out} is the output voltage, T is the switching period, and N_S and N_P are secondary and primary turns, respectively. The ZVS is achieved for load currents above the critical value.

$$I_2 > I_{crit}. \quad (6)$$

By substituting I_2 from (5) in (6), $I_{o,crit}$ is:

$$I_{o,crit} = \frac{N_P}{N_S} I_{crit} - \frac{\Delta I_o}{2} + \frac{V_{out}}{L_f} (1 - D) \frac{T}{2} \quad (7)$$

C. Switching Losses of MOSFETs

The switching power losses, including turn-on and turn-off losses are due to voltage and current cross over during switching transitions [17]. These losses are directly related to the switching frequency based on equations (8) and (9). The turn-off loss of a MOSFET is:

$$P_{off} = \frac{1}{2} V_{DS} I_{D(off)} t_{off} f_s \quad (8)$$

where, V_{DS} is the drain-source voltage, $I_{D(off)}$ is the drain current of a MOSFET during turn-off time, and t_{off} is the

turn-off time of a MOSFET. The turn-on loss of a MOSFET can be obtained as:

$$P_{on} = \frac{1}{2} V_{DS} I_{D(on)} t_{on} f_s \quad (9)$$

here, $I_{D(on)}$ is the drain current of a MOSFET during turn-on time, and t_{on} its turn-on time. It is obvious that a linear relationship exists between the frequency and switching losses. As the dominant switching losses are due to turn-on and turn-off losses of the switches, in light load conditions in which VFPWM is employed, turn-on and turn-off losses decrease due to low switching frequency. As the load increases, control mode is changed from VFPWM to ZVS mode, and thus switching losses significantly reduce.

D. Control Strategy

In the proposed method, VFPWM is employed in output currents less than $I_{o,crit}$ and ZVS is used in output currents more than $I_{o,crit}$ to achieve higher efficiency of the converter. Therefore, high efficiency is attained in a wide range of load variations. Fig. 3 shows the transition point of the proposed switching control method.

The magnetic flux density of the transformer is [18], [19]:

$$B_{tran} = \frac{V_{in} D}{4f_s A_e N_P} \quad (10)$$

where, A_e is the cross-sectional area of the transformer. In VFPWM mode, D and f_s in each control period should be determined such that, the ratio D/f_s stays constant at all output voltages. In VFPWM, f_s is changed from f_{min} to f_{max} and f_{min} is selected to satisfy (11) at the lowest demanding output voltage, that is 1V (t_{on} and t_{off} are used from data sheet of MOSFETs).

$$DT_s > 5(t_{on} + t_{off}). \quad (11)$$

Equations (12) and (13) express the relationship between the duty cycle of switches (D) and frequency (f) as the independent and dependent variable, respectively.

$$D = \frac{I_{in} N_S}{I_o N_P} \quad (12)$$

$$f - f_{max} = m(D - D_{max}) \quad (13)$$

here, f_{max} and D_{max} and m are constant. In VFPWM, if the output current is changed by a user, a new duty cycle is calculated from (12), and thus a new switching frequency is determined according to (13).

III. SIMULATION AND RESULTS

Table I presents the specifications of the considered converter. This converter converts fixed input voltage of 400V to the variable output voltage from 0 to 75V according to user demand. Based on the proposed control strategy, the converter works in the VFPWM mode in output currents less than $I_{o,crit} = 18A$. As the load current is more than 18A, control mode changes to ZVS mode. Thus, the converter can provide high efficiency in a wide range of output power.

TABLE I
SPECIFICATIONS

Item	Symbol	Value
Input Voltage	V_{in}	400V
Output Voltage	V_{out}	0-75V
Output Current	I_{out}	0-25A
Nominal Output Power	P_{out}	1875W
Turns Ratio	$N_p:N_s:N_s$	3.8:1:1
Magnetization Inductance	L_M	1.8mH
Leakage Inductance	L_{lk}	25 μ H [17]
Critical Output Current	$I_{o,crit}$	18A
Transformer winding capacitance	C_T	100pF [17]

TABLE II
VFPWM MODE FREQUENCY AND DUTY CYCLE IN DIFFERENT OUTPUT CURRENTS.

I_{out} (A)	Frequency (kHz)	Duty cycle (%)
2.7	11.21	2.5
4.4	11.81	5
7.7	13.2	10
11	15	15
18	21	25

Table II shows the VFPWM mode frequency and duty cycle in different output currents. Based on (11), $f_{min} = 10kHz$. By changing I_o from 0 to $I_{o,crit} = 18A$, duty cycle and frequency of switches change respectively. As it can be seen in Table II, $f_{max} = 21kHz$ and $D_{max} = 25\%$.

Fig. 4 shows the ZVS waveforms of the proposed technique in transition point and full load. Fig. 4a and Fig. 4c show voltages of MOSFET Q_2 and transformer primary side current I_{pri} in $I_o = 18A$, respectively. From this point, ZVS mode is attainable and all MOSFETs are under ZVS control mode. Thus, the turn-on loss of MOSFETs is almost zero and higher efficiency is obtained. Fig. 4b and Fig. 4d show ZVS waveforms at full load ($I_o = 25A$).

To validate the calculations, a comparison between three control methods - the variable frequency (VF) control method, the fixed frequency (FF) control method, and the proposed control method - is made in Fig.5. In the FF control method, f_s is 21kHz in all output currents. In the VF control method, frequency is variable from 10kHz to 21kHz and duty cycle of switches changes from 0 to 45% based on the linear relationship between frequency and duty cycle mentioned in part D. In low output powers, the efficiency is almost high and the output power versus efficiency curve is nearly flat. In low output currents, the efficiency of the VF control method is higher than the FF control method. However, with increasing output power, efficiency of the VF method decreases, as losses due to magnetic parts become more dominant and turn-on losses of the switches increase linearly with frequency. Therefore, the proposed control method which is the combination of VFPWM and ZVS control modes, uses the advantages of both the VF in low loads and the ZVS control method in high loads. The proposed method uses VFPWM in light loads where the zvs is

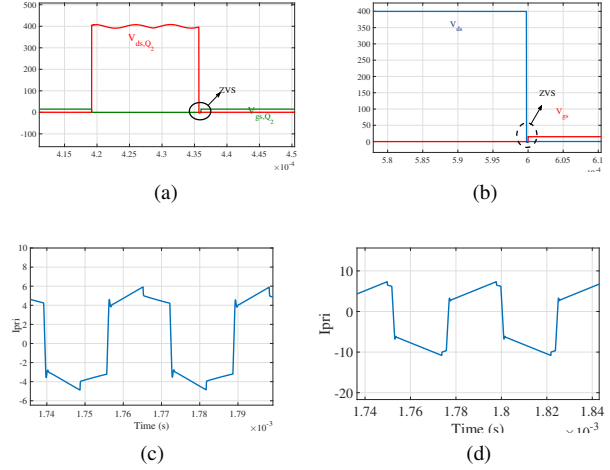


Fig. 4. (a) Gate-source voltage of Q_2 (V_{gs}) and drain-source voltage (V_{ds}) in $I_o = 18A$. (b) Gate-source voltage (V_{gs}) and drain-source voltage (V_{ds}) of Q_2 in full load. (c) Transformer primary side current in $I_o = 18A$. (d) Transformer primary side current I_{pri} in full load.

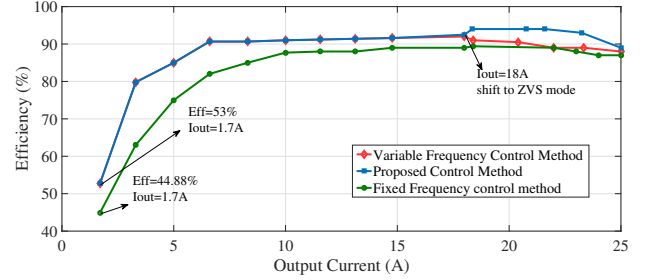


Fig. 5. Simulation results of efficiency curves with three different switching control modes $R_L = 3\Omega$.

hardly achieved and provide higher efficiency than FF in this range. Both curves of VF and proposed control method are the same until $I_o = 18A$ which is the minimum output current at which ZVS is attainable. From this point, the efficiency curve of the proposed control method increases dramatically, as the ZVS mode provides zero turn-on switching losses for MOSFETs. As it can be seen, using the proposed control strategy, the higher efficiency is obtained in a wide range of output power.

IV. CONCLUSION

This paper proposed a new hybrid control method for a full bridge DC/DC converter suitable for cathodic protection applications. The switching control modes of the proposed switching control technique are summarized as follows:

- Under heavy-load condition: Phase-shift switching control is employed to achieve zero voltage switching (ZVS) and thus lower power losses.
- Under light-load condition: Pulse-width-modulation switching control with variable frequency (VFPWM) is used to reduce switching losses and improve efficiency.

In this converter, user can change output current according to the CP requirements of the environment. The analytical forms for the losses and the transition point between modes for full-bridge converter and results from the simulations were presented and discussed. The proposed method can be used in different applications, where a variable output power in a wide range with a high efficiency is needed.

REFERENCES

- [1] R. W. Revie, *Corrosion and corrosion control: an introduction to corrosion science and engineering*. John Wiley & Sons, 2008.
- [2] J. P. Broomfield, *Corrosion of steel in concrete: understanding, investigation and repair*. CRC Press, 2006.
- [3] D.-D. Tran, H.-N. Vu, S. Yu, and W. Choi, "A novel soft-switching full-bridge converter with a combination of a secondary switch and a nondissipative snubber," *IEEE Transactions on Power Electronics*, vol. 33, no. 2, pp. 1440–1452, 2017.
- [4] Y. Shi and X. Yang, "Zero-voltage switching pwm three-level full-bridge dc-dc converter with wide zvs load range," *IEEE Transactions on Power Electronics*, vol. 28, no. 10, pp. 4511–4524, 2012.
- [5] L.-C. Shih, Y.-H. Liu, and H.-J. Chiu, "A novel hybrid mode control for a phase-shift full-bridge converter featuring high efficiency over a full-load range," *IEEE Transactions on Power Electronics*, vol. 34, no. 3, pp. 2794–2804, 2018.
- [6] W.-J. Lee, C.-E. Kim, G.-W. Moon, and S.-K. Han, "A new phase-shifted full-bridge converter with voltage-doubler-type rectifier for high-efficiency pdp sustaining power module," *IEEE Transactions on Industrial Electronics*, vol. 55, no. 6, pp. 2450–2458, 2008.
- [7] H. Wu, J. Zhang, X. Qin, T. Mu, and Y. Xing, "Secondary-side-regulated soft-switching full-bridge three-port converter based on bridgeless boost rectifier and bidirectional converter for multiple energy interface," *IEEE Transactions on Power Electronics*, vol. 31, no. 7, pp. 4847–4860, 2015.
- [8] D.-Y. Kim, C.-E. Kim, and G.-W. Moon, "Variable delay time method in the phase-shifted full-bridge converter for reduced power consumption under light load conditions," *IEEE Transactions on Power Electronics*, vol. 28, no. 11, pp. 5120–5127, 2013.
- [9] B.-Y. Chen and Y.-S. Lai, "Switching control technique of phase-shift-controlled full-bridge converter to improve efficiency under light-load and standby conditions without additional auxiliary components," *IEEE transactions on power electronics*, vol. 25, no. 4, pp. 1001–1012, 2009.
- [10] C.-E. Kim, "Optimal dead-time control scheme for extended zvs range and burst-mode operation of phase-shift full-bridge (psfb) converter at very light load," *IEEE Transactions on Power Electronics*.
- [11] K. R. Sree and A. K. Rathore, "Hybrid modulated extended secondary universal current-fed zvs converter for wide voltage range: Analysis, design, and experimental results," *IEEE Transactions on Industrial Electronics*, vol. 62, no. 7, pp. 4471–4480, 2014.
- [12] H. Wu, T. Mu, H. Ge, and Y. Xing, "Full-range soft-switching-isolated buck-boost converters with integrated interleaved boost converter and phase-shifted control," *IEEE Transactions on Power Electronics*, vol. 31, no. 2, pp. 987–999, 2015.
- [13] S.-Y. Cho, I.-O. Lee, J.-K. Kim, and G.-W. Moon, "A new standby structure based on a forward converter integrated with a phase-shift full-bridge converter for server power supplies," *IEEE Transactions on Power Electronics*, vol. 28, no. 1, pp. 336–346, 2012.
- [14] J.-H. Kim, C.-E. Kim, J.-K. Kim, J.-B. Lee, and G.-W. Moon, "Analysis on load-adaptive phase-shift control for high efficiency full-bridge llc resonant converter under light-load conditions," *IEEE Transactions on Power Electronics*, vol. 31, no. 7, pp. 4942–4955, 2015.
- [15] N. Hassanzadeh, F. Yazdani, S. Haghbin, and T. Thiringer, "Design of a 50 kw phase-shifted full-bridge converter used for fast charging applications," in *2017 IEEE Vehicle Power and Propulsion Conference (VPPC)*. IEEE, 2017, pp. 1–5.
- [16] J. Sabate, V. Vlatkovic, R. Ridley, F. Lee, B. Cho *et al.*, "Design considerations for high-voltage high-power full-bridge zero-voltage-switched pwm converter," in *Proc. IEEE APEC*, vol. 90, 1990, pp. 275–284.
- [17] Z. Chen, S. Liu, L. Shi, and F. Ji, "A power loss comparison of two full bridge converters with auxiliary networks," in *Proceedings of The 7th International Power Electronics and Motion Control Conference*, vol. 3. IEEE, 2012, pp. 1888–1893.
- [18] L. Zhao, H. Li, Y. Liu, and Z. Li, "High efficiency variable-frequency full-bridge converter with a load adaptive control method based on the loss model," *Energies*, vol. 8, no. 4, pp. 2647–2673, 2015.
- [19] N. Mohan and T. M. Undeland, *Power electronics: converters, applications, and design*. John Wiley & sons, 2007.